

NEAR-INFRARED SPECTROSCOPY AND *HUBBLE SPACE TELESCOPE* IMAGING OF A DUSTY STARBURST ERO¹

GRAHAM P. SMITH,^{2,3} TOMMASO TREU,⁴ RICHARD ELLIS,⁴ IAN SMAIL,² J.-P. KNEIB⁵ & B. L. FRYE.⁶

Received 2001 – –; Accepted: 2001 – –

ABSTRACT

We present near-infrared spectroscopy and *Hubble Space Telescope* (*HST*) imaging of ERO J164023+4644, an Extremely Red Object (ERO) with $(R-K) = 5.9$ at $z = 1.05$ that has been detected by *ISO* at $15\mu\text{m}$. ERO J164023 appears to be a disk galaxy, with an optical/infrared spectral energy distribution which appears to be strongly reddened by dust ($L_{\text{FIR}}/L_{\text{B}} \lesssim 200$; $A_{\text{V}} \sim 5$). The combination of the narrow width of the emission lines in our spectra ($\sim 300\text{km s}^{-1}$) and the relatively high $[\text{NII}]/\text{H}\alpha$ line ratio indicate that this is a “composite” starburst-Seyfert galaxy. Assuming that star formation dominates the energy output, we constrain the star formation rate to lie in the broad range $\sim 10\text{--}700\text{M}_{\odot}\text{yr}^{-1}$ from a variety of star formation indicators. We compare ERO J164023 with the only other spectroscopically identified dusty EROs: HR10 ($z = 1.44$) and ISO J1324–2016 ($z = 1.50$). ERO J164023 and HR10 have similar disk-like morphologies in the rest frame UV, and both exhibit a variation in the apparent dust obscuration depending upon the diagnostic used which suggests that there is a complex spatial mix of stellar populations and dust in these galaxies. In contrast, the compact morphology and spectral properties of ISO J1324–2016 indicate that it is a dusty quasar. Overall, our results demonstrate that the population of dusty galaxies identified using photometric ERO criteria includes systems ranging from pure starbursts, through transition systems such as ERO J164023 to dusty quasars. We suggest that the classification of EROs into these sub-classes, necessary for the detailed modelling of the population, cannot be reliably achieved from optical/near-infrared photometry and instead requires mid/far-infrared or sub-millimetre photometry and near-infrared spectroscopy. The advent of efficient multi-object spectrographs working in the near-infrared as well as the imminent launch of *SIRTF* therefore promise the opportunity of rapid progress in our understanding of the elusive ERO population.

Subject headings: galaxies: individual; ERO J164023+4644.0 — galaxies: evolution — galaxies: starburst — infrared: galaxies

1. INTRODUCTION

Our understanding of both the star formation history of the Universe and emission from active galactic nuclei (AGN) was challenged in the late-1990s by mid-infrared (MIR) (e.g. Rowan-Robinson et al. 1997; Flores et al. 1999) and sub-millimetre (sub-mm) (Smail et al. 1997, 2001; Eales et al. 1999; Dunlop 2001) observations of luminous far-infrared (FIR) galaxies at high redshift. If, as has been suggested, the FIR emission from these galaxies arises from star formation then these observations suggest that around half of all star formation may have occurred in highly obscured systems (Blain et al. 1999; Elbaz et al. 1999). Tracing the evolution of dust-obscured star-formation and AGN-activity as a function of cosmic epoch is therefore essential to our understanding of galaxy evolution.

The identification of the optical counterparts of these sub-mm and MIR sources is not straightforward due to the optical faintness of many of the candidates and the large positional uncertainties in the longer wavelength observations ($\sim 3\text{--}4''$). Nevertheless, where counterparts are found, many of these appear to be red in optical passbands, with some being extremely red objects (EROs) with $(R-K) > 6$ (Smail et al. 1999; Gear et

al. 2000). Whilst it is possible for such colors to be produced by evolved stellar populations at $z \gtrsim 1$, the intense FIR emission of these galaxies suggests that dust is also likely to be responsible for their extreme colors.

Recent imaging observations suggest that up to 20–50 per cent of all EROs with $(R-K) \geq 5.3$ and the majority of those with $(R-K) \geq 6.0$ may be dusty starburst galaxies (Smail et al. 1999; Treu & Stiavelli 1999; Moriondo et al. 2000; Smith et al. 2001). However, to understand more about the nature of these galaxies requires spectroscopic study. Such observations are extremely challenging, even with 10-m class telescopes, due to the optical faintness of EROs ($R \gtrsim 24$). Consequently, only two dusty EROs have been spectroscopically identified to date: HR10, a starburst galaxy at $z = 1.44$ (Dey et al. 1999 - hereafter D99) and ISO J1324–2016, a dusty AGN at $z = 1.50$ (Pierre et al. 2001).

To drive forward this field Smith et al. (2001, hereafter S01) recently exploited the magnifying power of ten massive galaxy cluster lenses to boost the sensitivity of follow-up spectroscopy of EROs. They combined ground-based NIR observations with deep *HST* optical imaging to construct a sample of 60 gravitationally lensed EROs. This paper presents the detailed follow-

¹Based on observations with the NASA/ESA *Hubble Space Telescope* obtained at the Space Telescope Science Institute, which is operated by the Association of Universities for Research in Astronomy Inc., under NASA contract NAS 5-26555.

²Department of Physics, University of Durham, South Road, Durham DH1 3LE, UK

³E-mail: graham.smith@durham.ac.uk

⁴Astronomy 105-24, Caltech, Pasadena CA 91125, USA

⁵Observatoire Midi-Pyrénées, CNRS-UMR5572, 14 Avenue E. Belin, 31400 Toulouse, France

⁶Lawrence Berkeley National Laboratory, Department of Physics, Mailstop 50-232, Berkeley, CA 94720

up of one source from this sample: ERO J164023+4644 (hereafter referred to as ERO J164023). This galaxy was previously associated with an *ISO* $15\mu\text{m}$ source by Barvainis et al. (1999), who tentatively identified a single optical emission line as [OII] at $z = 1.05$, although they did not realise that the galaxy is an ERO.

We describe our observations in §2 and present our results in §3. We compare ERO J164023 with HR10 and ISO J1324–2016 in §4 and summarise our conclusions in §5. We assume $H_0 = 50\text{km s}^{-1}\text{Mpc}^{-1}$, $\Omega_0 = 1$ and $\Lambda_0 = 0$ and adopt a lens amplification of 1.4 for ERO J164023 (S01).

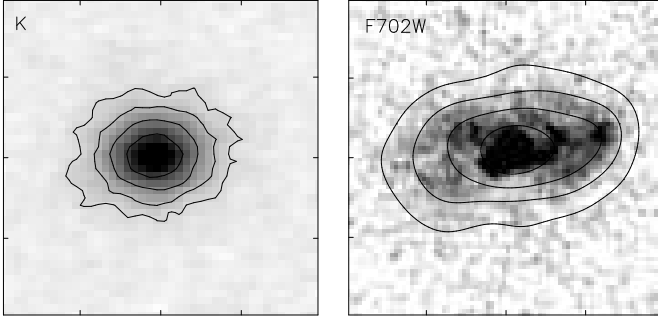


FIG. 1. — The UKIRT *K*-band (left) and *HST* F702W (right) images of ERO J164023. The resolution of these two images is $\sim 0.5''$ and $\sim 0.1''$ respectively. The contours on the left-hand panel are from the raw *K*-band image that also appears as the gray-scale in this panel and the contours in the right-hand panel are from the seeing-matched (i.e. $\sim 0.5''$ resolution) *HST* frame. The tick marks are $1''$ apart; North is up and East is Left.

2. OBSERVATIONS

2.1. Imaging

The *K*-band data used to identify ERO J164023 was obtained in a 6.5-ks exposure using the UFTI imager on the 3.8-m UK Infrared Telescope⁷ (UKIRT) in $0.5''$ seeing on 2000 April 5 (S01). ERO J164023 lies at 16:40:23.05 +46:44:02.3 (J2000) and a *K*-band image of this galaxy is shown in Fig. 1.

In addition to the *K*-band imaging, we obtained a *J*-band image of ERO J164023 with INGRID on the 4.2-m William Herschel Telescope (WHT)⁸ on 2001 May 6. This observation totalled 2.2 ks in $\sim 0.8''$ seeing, and was reduced in a similar manner to the *K*-band data. We also exploit *H*-band observations of this field from Gray et al. (2000) using CIRSI on the WHT.

Morphological information on the ERO comes from *HST* imaging of the cluster. The field containing ERO J164023, A 2219, was observed with *WFPC2* onboard *HST* for six exposures totalling 14.4 ks through the F702W filter (S01). We show the *WFPC2* image of this galaxy in Fig. 1. To obtain optical photometry of the field we have also analysed archival *UBVI*-band imaging of A 2219 taken with COSMIC on the Hale 5-m⁹ and LRIS on Keck¹⁰ (Smail et al. 1995, 1998).

Mid-infrared observations of the galaxy come from Barvainis et al. (1999) who observed A 2219 at $15\mu\text{m}$ with *ISOCAM* on-board ESA's *Infrared Space Observatory* (*ISO*). They detected five sources, one of which (A2219#5) lies within $\sim 0.8''$ of ERO J164023.

At longer wavelengths, A 2219 was also observed by Chapman et al. (2000) using SCUBA at $850\mu\text{m}$ (Holland et al. 1999) on the 15-m James Clerk Maxwell Telescope¹¹.

⁷The United Kingdom Infrared Telescope is operated by the Joint Astronomy Centre on behalf of the Particle Physics and Astronomy Research Council

⁸The William Herschel Telescope is operated by the Isaac Newton Group on behalf of Particle Physics & Astronomy Research Council

⁹The Hale Telescope at Palomar Observatory is owned and operated by the California Institute of Technology

¹⁰The W. M. Keck Observatory which is operated as a scientific partnership between Caltech, the University of California and NASA

¹¹The James Clerk Maxwell Telescope is operated by the JAC on behalf of the Particle Physics & Astronomy Council, the Netherlands Organisation for Scientific Research and the National Research Council of Canada

They tentatively identified one of the sources in this field (SMM J16404+4644) with A2219#5 from Barvainis et al. (1999). However, as the $850\mu\text{m}$ source is $\gtrsim 6''$ away from ERO J164023, we suggest that this identification is probably incorrect and instead we adopt Chapman et al.'s $3\text{-}\sigma$ detection as a conservative upper limit on the $850\mu\text{m}$ flux from ERO J164023.

Finally, we obtain $3\text{-}\sigma$ detection limits in the radio from the 28.5 GHz, 4.9 GHz, 1.4 GHz maps of Cooray et al. (1998), Edge (private communication) and Owen (private communication). We list our optical, infrared, sub-millimeter and radio photometry in Table 1.

TABLE 1
PHOTOMETRY OF ERO J164023

| Observed Band | Flux Density ^{a,c} (μJy) | Magnitude ^{b,c} | Reference |
|------------------|---|--------------------------|------------------------------|
| <i>U</i> | < 0.10 | > 25.6 | Smail et al. (1998) |
| <i>B</i> | 0.13 ± 0.02 | 26.2 ± 0.1 | Smail et al. (1998) |
| <i>V</i> | 0.19 ± 0.03 | 25.7 ± 0.2 | Smail et al. (1995) |
| <i>R</i> | 1.32 ± 0.05 | 23.54 ± 0.04 | S01 |
| <i>I</i> | 3.00 ± 0.24 | 22.15 ± 0.08 | S01 |
| <i>J</i> | 20.4 ± 0.6 | 19.72 ± 0.06 | This paper |
| <i>H</i> | 21.3 ± 0.7 | 19.20 ± 0.09 | Gray et al. (2000) |
| <i>K</i> | 63.0 ± 0.6 | 17.64 ± 0.01 | S01 |
| $15\mu\text{m}$ | 530 ± 110 | ... | Barvainis et al. (1999) |
| $850\mu\text{m}$ | $< 6 \times 10^3$ | ... | Chapman et al. (2000) |
| 28.5 GHz | < 780 | ... | Cooray et al. (1998) |
| 4.9 GHz | < 300 | ... | Edge (private communication) |
| 1.4 GHz | < 100 | ... | Owen (private communication) |

^a Errors quoted are $1\text{-}\sigma$. Limits quoted are $3\text{-}\sigma$ detection limits.

^b All magnitudes are measured in a $2''$ diameter aperture.

^c Flux density measurements and magnitudes in this table have not been corrected for gravitational amplification by the foreground cluster lens, A 2219.

2.2. Spectroscopy

A NIR spectrum of ERO J164023 was obtained in the *J*-band with NIRSPEC on Keck-II on 2001 April 9 in photometric conditions and $0.6''$ seeing. Three exposures of 600 s each were obtained, nodding along the $0.76'' \times 42''$ slit by $5''$ between each exposure. The resolution of these observations was 10 Å FWHM.

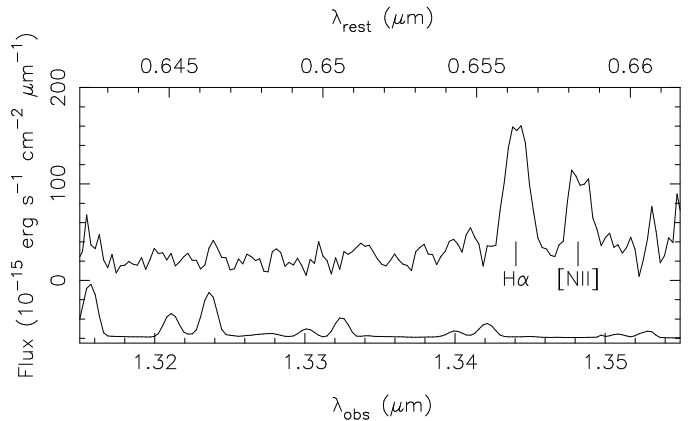


FIG. 2. — The near-infrared spectrum of ERO J164023. We identify the strong emission lines as $\text{H}\alpha$ $\lambda 6563$ and $[\text{NII}]\lambda 6583$, giving a redshift of $z = 1.0480 \pm 0.0005$.

Wavelength calibration was achieved from the sky lines, using observations of a bright star to correct for geometrical distortion. An average sky spectrum was created by scaling and

combining the individual spectra and this was then subtracted from each science observation before co-adding the spectra and extracting a one-dimensional spectrum. Flux calibration was achieved through observations of UKIRT standard stars, which were also used to correct for telluric absorption. No attempt was made to correct for slit losses.

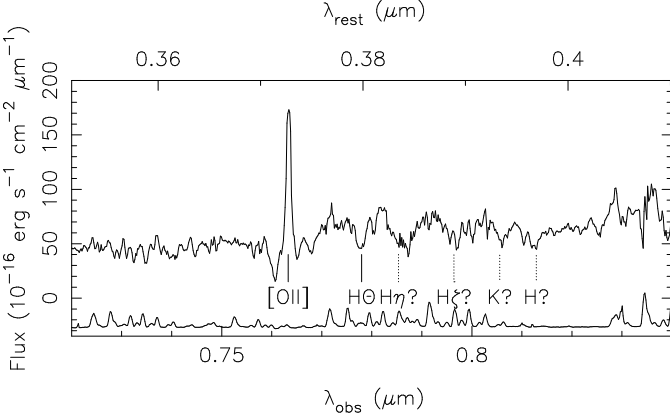


FIG. 3. — The optical spectrum of ERO J164023. We identify the strong emission line as [OII]λ3727 which is confirmed by the identification of the Hα and [NII] lines in the NIR spectrum (Fig. 2). The Hθ absorption feature is also tentatively detected, although other members of the Balmer series and the Ca H and Ca K features are not visible. The sky spectrum is also shown in arbitrary units below the science spectrum.

The flux-calibrated spectrum (Fig. 2) reveals two strong emission lines at 1.3441 and 1.3483 μm, which we identify as Hα, and [NII]λ6583 respectively. This places the galaxy at a redshift of $z = 1.0480 \pm 0.0005$.

Barvainis et al. (1999) discuss an optical spectrum of A2219#5 (§2.1) obtained by Frye & Broadhurst using LRIS on Keck-I which is shown in Fig. 3. This shows a strong emission line at 7634 Å which Barvainis et al. tentatively identified as [OII]λ3727 at a redshift of $z = 1.048$, as confirmed by our NIR spectrum. The optical spectrum also appears to contain the Hθ absorption feature, although other members of the Balmer series and the Ca H & K lines are not convincingly detected. We present the emission line measurements in Table 2.

TABLE 2
EMISSION LINE MEASUREMENTS OF ERO J164023

| Line | λ_{obs} (μm) | Flux ^a (10^{-17} erg s $^{-1}$ cm $^{-2}$) | FWHM ^{a,b} (km s $^{-1}$) | $W_{\lambda, rest}^a$ (Å) |
|-------|-------------------------|--|--|------------------------------|
| [OII] | 0.7632 | 2 ± 1 | < 320 | 30 ± 5 |
| Hα | 1.3441 | 27 ± 2 | 310 ± 50 | 60 ± 15 |
| [NII] | 1.3483 | 18 ± 2 | 330 ± 50 | 50 ± 20 |

^a Fluxes, equivalent widths, and FWHMs are measured by fitting a Gaussian using SPLAT in IRAF and are not corrected for gravitational amplification.

^b FWHM measurements are quoted after correcting for the instrumental resolution of the spectrograph.

3. RESULTS AND DISCUSSION

3.1. Morphology

The *HST* frame ($\sim 0.1''$ resolution) suggests that ERO J164023 has a disk morphology in the rest frame UV (Fig. 1), with no obvious signs of strong dynamical disturbance. The disk component is sufficiently extended, $\sim 2\text{--}3''$ (10–15 kpc), that it remains visible when the *HST* frame is degraded to the ground-based resolution (0.5''). In contrast, at this resolution the *K*-band emission shows less evidence of a disk and is more concentrated. The $(R-K) \sim 6$ color of ERO J164023 (Table 1) is dominated by its central regions,

with the outer regions displaying a more “modest” optical/NIR colour of $(R-K) \sim 5.3$.

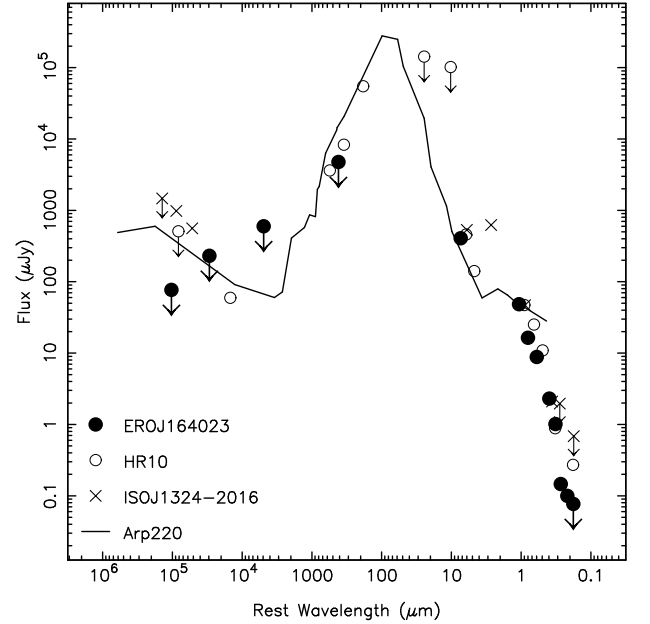


FIG. 4. — The rest frame spectral energy distribution (SED) of ERO J164023 from optical to radio wave-bands. For comparison, we show the SEDs of HR10 (D99; Elbaz et al. 2001), ISO J1324–2016 (Pierre et al. 2001) and Arp220 (Hughes et al. 1998). The flux densities of ERO J164023 have all been corrected for gravitational amplification (§1). The SEDs of all four galaxies have been normalised to the observed *K*-band flux of ERO J164023.

3.2. Spectral Energy Distribution

We plot the rest frame spectral energy distribution (SED) of ERO J164023 in Fig. 4. The SED of ERO J164023 rises steeply at optical/MIR wavelengths and, although less well-constrained at sub-mm/radio wavelengths, the flux density probably peaks in the FIR/sub-mm.

The extreme redness of the SED at optical/NIR/MIR wavelengths, suggests that the spectrum of ERO J164023 is heavily reddened by dust. We quantify this in two ways, first using the rest-frame FIR-to-blue luminosity ratio (L_{FIR}/L_B). We estimate the (unlensed) FIR luminosity of ERO J164023, using the 850 μm flux limit (Table 1) to scale the FIR luminosity of HR10 (D99), obtaining $L_{FIR} \lesssim 4 \times 10^{12} L_{\odot}$, and we measure the (unlensed) rest-frame blue luminosity to be $L_B \sim 2 \times 10^{10} L_{\odot}$ by interpolating between the observed *I*- and *J*- bands (Table 1). We therefore estimate $L_{FIR}/L_B \lesssim 200$. Second, we use HYPER-Z (Bolzonella et al. 2000) to investigate the SED of ERO J164023 by fitting template star-forming model spectra for a range of star formation ages and dust extinction to the photometric data presented in Table 1. Assuming a starburst age of < 0.2 Gyr and adopting the spectroscopic redshift ($z = 1.048$) produces a solution of $A_V \sim 5$, confirming that ERO J164023 is heavily dust-obscured.

3.3. Starburst or AGN?

The spectra of ERO J164023 (Fig. 2) contains narrow [OII], Hα and [NII] emission lines (Table 2) and a weak Hθ absorption feature. These spectral features are all more typical of star forming galaxies than AGN (e.g. Liu & Kennicutt 1995).

However, the [NII] to Hα flux ratio, $\log([NII]/H\alpha) \sim -0.2$ (Table 2), is higher than the typical value (-0.5) seen for star forming galaxies and suggests that the ERO may be a Seyfert 2 (Veilleux & Osterbrock 1987) or more likely, a composite

starburst-Seyfert galaxy (Hill et al. 1999). Nevertheless, the nuclear activity in ERO J164023 may be quite weak, as an AGN contribution to the line emission of as little as 10 per cent appears to be sufficient to account for the [NII] to $H\alpha$ ratio (Hill et al. 2001). We also note that ERO J164023 was not detected when A2219 was observed at X-ray wavelengths by *ROSAT* *HRI*, implying that any AGN is not X-ray bright. The $3\text{-}\sigma$ detection limit from these observations is $< 5.7 \times 10^{-4} \mu\text{Jy}$ [0.1–2.4 keV] (Edge, private communication).

Assuming that star formation dominates the line emission, we estimate the star formation rate (SFR) of ERO J164023 from its lensing-corrected $H\alpha$ luminosity: $L_{H\alpha} = 3.3 \times 10^8 L_{\odot}$, obtaining $\text{SFR}_{H\alpha} \sim 10 M_{\odot} \text{yr}^{-1}$ for a Salpeter IMF (Kennicutt 1998). As we have made no corrections for dust extinction, this is probably a lower limit. Indeed, a suppression of the observed line fluxes due to dust is also suggested by the very low [OII] to $H\alpha$ flux ratio of ERO J164023 (0.07 ± 0.03 , Table 2), which is far lower than the value seen in nearby spirals, 0.43 ± 0.27 , and more typical of local dusty starburst galaxies (Poggianti & Wu 2000).

The constraints on the luminosity of the ERO at longer wavelengths can also be used to place an upper limit on the probable star formation rate. Based on the lensing-corrected far-infrared luminosity of $L_{\text{FIR}} \lesssim 4 \times 10^{12} L_{\odot}$, we estimate $\text{SFR}_{\text{FIR}} \lesssim 700 M_{\odot} \text{yr}^{-1}$ (Kennicutt 1998). A similar upper limit to the SFR is obtained based on the 1.4 GHz flux limit (Table 1). We therefore can only constrain the SFR of ERO J164023 to lie within a broad range: $\sim 10\text{--}700 M_{\odot} \text{yr}^{-1}$, although all of the estimates suggest that this is a strongly star forming galaxy. The factor of 70 difference between the FIR and $H\alpha$ estimates of the SFR is consistent with that found by Poggianti & Wu (2000) for local starburst galaxies, indicating that the SFR could feasibly be as high as $\sim 700 M_{\odot} \text{yr}^{-1}$.

4. THE DUSTY ERO POPULATION

We now compare the properties of ERO J164023 with the only other spectroscopically-confirmed dusty EROs: the $z = 1.44$ starburst galaxy, HR10 (D99), and the dusty quasar ISO J1324–2016 at $z = 1.50$ (Pierre et al. 2001).

We start by classifying the EROs using the $(I-K)$ – $(J-K)$ diagnostic diagram suggested by Pozzetti & Mannucci (2000). Unfortunately, there is no published J -band photometry for ISO J1324–2016, but using the $(I-K)$ and $(J-K)$ colors of ERO J164023 (4.5 ± 0.1 and 2.1 ± 0.1 ; S01) and HR10 (5.8 ± 0.1 and 2.6 ± 0.1 ; D99) we find that these galaxies both lie just on the starburst side of the proposed dividing line between evolved and starburst EROs on the $(I-K)$ – $(J-K)$ plane. However, due to the photometric uncertainties, neither ERO can be robustly classified as a starburst on the basis of these three photometric bands alone.

To compare the three EROs across a broader wavelength range we plot the SEDs of HR10 and ISO J1324–2016 in Fig. 4. Dealing first with HR10 – the spectral shapes of ERO J164023 and HR10 at optical/NIR/MIR wavelengths are very similar and both resemble the SED of Arp 220, implying that both galaxies are highly obscured. D99 estimate $L_{\text{FIR}}/L_B \sim 300$ for HR10, suggesting that it may be more heavily obscured than ERO J164023. On the other hand, the crude estimates of dust obscuration from the V -band extinction and [OII]/ $H\alpha$ line ratio suggest that ERO J164023 and HR10 suffer comparable degrees of dust obscuration. The scatter seen in the estimates of the relative extinction in these two systems depending upon the diagnostic used supports the idea that the dust has a complex

spatial distribution and produces different degrees of obscuration for the emission from the various stellar populations within the galaxies (e.g. Poggianti & Wu 2000).

There is some morphological support for differences in the spatial distribution of visible stars and dust in both HR10 and ERO J164023. *HST* imaging of HR10 in the F814W filter is discussed by D99, the higher redshift of this ERO means that these observations sample similar rest frame UV wavelengths to the F702W image of ERO J164023 ($\sim 3500\text{\AA}$). HR10 displays an “S”-shaped morphology, suggesting that it is a disk galaxy, although D99 propose that it may be dynamically disturbed. In contrast, the K -band morphology of HR10 is more symmetrical, suggesting that, like ERO J164023, it may either harbor a bulge of older stars, or more likely a central starburst that is more heavily dust-reddened than the outskirts of the galaxies.

D99 propose that HR10 is a dusty starburst-powered galaxy based on the lack of signatures of nuclear activity in both its emission line widths ($\sim 600 \text{ km s}^{-1}$) and its emission line ratio: $\log([\text{NII}]/H\alpha) \sim -0.4$. Applying the same conversions as used in §3.3, we estimate the SFR in HR10 lies in the range $\sim 40\text{--}1200 M_{\odot} \text{yr}^{-1}$, where the lower bound again comes from the observed $H\alpha$ flux (uncorrected for dust) and the upper bound is based on the FIR luminosity of the galaxy. This range suggests that HR10 may be forming stars at a rate $\sim 2\text{--}3$ times higher than ERO J164023.

Turning now to the comparison of ERO J164023 with ISO J1324–2016, we see that in contrast to the broad similarities between ERO J164023 and HR10, the galaxy shares few characteristics with ISO J1324–2016. The lack of *HST* imaging of ISO J1324–2016 precludes detailed analysis of its morphology, however Pierre et al. (2001) state that this source appears point-like in $\sim 0.5''$ seeing in the K -band, unlike ERO J164023 (and HR10) which is extended in similar seeing at these wavelengths (Fig. 1). The optical SED of ISO J1324–2016 also shows the precipitous decline in the UV characteristic of reddening by dust (Pierre et al. (2001) estimate $A_V \sim 4\text{--}7$ from the Balmer decrement in ISO J132402916), however the behaviour in the mid-infrared is very different from ERO J164023 (and HR10) with excess emission at $6.75 \mu\text{m}$, which has been interpreted as evidence for a hot component, probably from circum-nuclear dust around an AGN.

The identification of ISO J1324–2016 as a dusty quasar is confirmed by a strong, broad $H\alpha$ emission line ($\sim 3000 \text{ km s}^{-1}$) and relatively strong radio emission ($P_{1.4\text{GHz}} \sim 2 \times 10^{25} \text{ W Hz}^{-1}$). This contrasts markedly with the narrow line widths seen in both ERO J164023 and HR10. In addition, neither ERO J164023, nor HR10, have so far been detected at 1.4 GHz, although both appear to be at least an order of magnitude less luminous than ISO J1324–2016 in this band, with $P_{1.4\text{GHz}} \lesssim 5 \times 10^{23}$ and $\lesssim 4 \times 10^{24} \text{ W Hz}^{-1}$ respectively.

In summary: the properties of ERO J164023 suggest it shares many characteristics with the ultraluminous starburst HR10, although it is less extreme and also shows evidence of nuclear activity. However, the AGN component in ERO J164023 is dominated in most observations by the star formation in this galaxy and hence this system differs markedly from the dusty quasar, ISO J1324–2016.

5. CONCLUSIONS

We have obtained a secure spectroscopic identification of ERO J164023, a dusty starburst-Seyfert ERO at a redshift of $z = 1.05$. This brings the total number of spectroscopically identified dusty EROs to three and adds a composite AGN/starburst

system to the apparently pure starburst (HR10) and AGN-dominated systems (ISO J1324–2016) previously identified.

We complement this spectroscopy with deep *HST* optical imaging and infrared, sub-mm and radio data, enabling us to study the morphology and SED of this unusual galaxy. The main conclusions of our work are as follows:

(i) ERO J164023 is a disk galaxy, the central region of which dominates its optical/NIR color of $(R-K) \sim 6$. The steep optical/IR SED is consistent with this galaxy being heavily obscured by dust ($L_{\text{FIR}}/L_B \lesssim 200$; $A_V \sim 5$).

(ii) The spectral line widths are consistent with the dust emission being powered by hot young stars. However, the $[\text{NII}]/\text{H}\alpha$ line strength ratio suggests that this is a “composite” starburst-Seyfert galaxy. Assuming star formation to be the dominant power source, we constrain the SFR to lie in the broad range $\sim 10\text{--}700 M_\odot \text{yr}^{-1}$ which is a factor of $\sim 2\text{--}3$ times lower than HR10.

(iii) ERO J164023 and HR10 have strikingly similar rest frame optical/NIR/MIR spectral properties and both exhibit disk-like morphologies. The dominant role of the central region of these galaxies in producing their extremely red optical/NIR colors is consistent with them both containing an obscured, central starburst. Variation of the measured dust obscuration suffered by each galaxy from a number of diagnostics suggests that the dust and various stellar populations within dusty starburst galaxies differ in their spatial distributions.

(iv) Despite the photometric similarities of the three EROs, HR10 and ERO J164023 both differ from ISO J1324–2016 in that the latter’s emission is primarily driven by an AGN, whereas star formation appears to be the power source in HR10 and ERO J164023.

Overall, our work reveals that samples of dusty EROs contain the full range of power sources: dusty starbursts, AGNs and composite starburst-AGN systems. The broad wavelength range of our imaging (X-ray to radio) together with our optical and NIR spectroscopy allows us to identify which observations

are required to accurately segregate active (i.e. dusty) and passive EROs and then to classify active EROs into their different sub-classes.

Firstly, whilst the $(I-K)-(J-K)$ color-color plane (Pozzetti & Mannucci 2000) provides a rough classification between active and passive EROs, photometric uncertainties appear to undermine the accuracy of this method (a concern shared by Pozzetti & Mannucci 2000). Accurate separation of active and passive EROs therefore requires MIR/FIR or submm observations to search for the signature dust emission of active systems. The forthcoming launch of *SIRTf* should provide the opportunity for rapid progress in this respect.

However, NIR spectroscopy is also essential to further classify active EROs into their respective sub-classes on the basis of their detailed spectral properties. Spectral analysis of a statistically reliable sample of active EROs is therefore crucial to a better understanding of the evolution of dust-obscured star formation and AGN-activity as a function of cosmic epoch. We anticipate that the forthcoming generation of NIR multi-object spectrographs will play a significant role in advancing our understanding of the elusive ERO population.

ACKNOWLEDGEMENTS

We are especially grateful to Roser Pelló for her assistance with the HYPER-Z analysis and Karl Glazebrook for help with the Keck observations. We are also grateful to Scott Chapman, Alastair Edge, Meghan Gray, Frazer Owen, for sharing their observational data with us. Thanks also go to Harald Ebeling, Rob Ivison, Harald Kuntschner, Alice Shapley and Chuck Steidel for a variety of invaluable discussions and assistance. GPS acknowledges a postgraduate studentship from PPARC. IRS acknowledges support from the Royal Society and the Leverhulme Trust. JPK acknowledges support from CNRS. We also acknowledge support from the UK–French ALLIANCE collaboration programme #00161XM.

REFERENCES

- Barvainis R., Antonucci R., Helou G., 1999, *AJ*, 118, 645
 Blain A.W., Smail I., Ivison R.J., Kneib J.-P., 1999, *MNRAS*, 302, 632
 Bolzonella M., Miralles J.M., Pelló, 2000, *A&A*, 363, 476
 Chapman S.C., Scott D., Borys C., Fahlman G.G., 2001, *MNRAS*, submitted (astro-ph/0009067)
 Cooray A.R., Grego L., Holzapfel W.L., Joy M., Carlstrom J.E., 1998, *AJ*, 115, 1388
 Dey A., Graham J.R., Ivison R.J., Smail I., Wright G.S., Liu M.C., 1999, *ApJ*, 519, 610 (D99)
 Dunlop J.S., 2001, in *UMass/INAOE Conference on Deep Millimeter Surveys*, eds. Lowenthal J., Hughes D., (astro-ph/0011007)
 Eales S.A., Lilly S.J., Gear W.K., Dunne L., Bond J.R., Hammer F., Le Fèvre O., Crampton D., 1999, *ApJ*, 515, 518
 Elbaz D., et al., 2001, *A&A*, submitted
 Flores H., Hammer F., Thuan T.X., Césarsky C., Desert F.X., Omont A., et al., 1999, *ApJ*, 517, 148
 Gear W.K., Lilly S.J., Stevens J.A., Clements D.L., Webb T.M., Eales S.A., Dunne L., 2000, *MNRAS*, 316, 51
 Gray M.E., Ellis R.S., Refregier A., Bežecourt J., McMahon R.G., Beckett M.G., Mackay C.D., Hoenig M.D., 2000, *MNRAS*, 318, 573
 Hill T.L., Heisler C.A., Sutherland R., Hunstead R.W., 1999, *AJ*, 117, 111
 Hill T.L., Heisler C.A., Norris R.P., Reynolds J.E., Hunstead R.W., 2001, 121, 128
 Holland W.S., Robson E.I., Gear W.K., Cunningham C.R., Lightfoot J.F., Jenness T., et al., 1999, *MNRAS*, 303, 659
 Hughes D.H., Dunlop J.S., 1998, in Carilli C., et al., eds, *ASP Conf. Ser.*, Highly Redshifted radio lines. Soc. Pac. San Francisco.
 Kennicutt R.C., 1998, *ARA&A*, 36, 189
 Liu C.T., Kennicutt R.C., 1995, *ApJ*, 450, 547
 Moriondo G., Cimatti A., Daddi E., 2000, *A&A*, 364, 26
 Pierre M., Lidman C., Hunstead R., Alloin D., Casali M., Cesarsky C., Chantal P., Duc P.-A., Fadda D., Flores H., Madden S., Vigroux L., 2001, *A&A*, submitted (astro-ph/0105075)
 Poggianti B.M., Wu H., 2000, *ApJ*, 529, 157
 Pozzetti L., Mannucci F., 2000, *MNRAS*, 317, L17
 Rowan-Robinson M., et al., 1997, *MNRAS*, 261, 513
 Smail I., Hogg D.W., Blandford R., Cohen J.G., Edge A.C., Djorgovski S.G., 1995, *MNRAS*, 277, 1
 Smail I., Ivison R.J., Blain A.W., 1997, *ApJ*, 490, 5
 Smail I., Edge A.C., Ellis R.S., Blandford R.D., 1998, *MNRAS*, 293, 124
 Smail I., Ivison R.J., Kneib J.-P., Cowie L.L., Blain A.W., Barger A.J., Owen F.N., Morrison G., 1999, *MNRAS*, 308, 1061
 Smail I., Ivison R.J., Blain A.W., Kneib J.-P., 2001, *MNRAS*, submitted
 Smith G.P., Smail I., Kneib J.-P., Czoske O., Ebeling H., Edge A.C., Pelló R., Ivison R.J., Packham C., Le Borgne J.-F., 2001, *MNRAS*, submitted (S01)
 Treu T., Stiavelli M., 1999, *ApJ*, 524, L27
 Veilleux S., Osterbrock D.E., 1987, *ApJS*, 63, 295